Alternating-Direction Implicit (ADI) Formulation of the Finite-Difference Time-Domain (FDTD) Method: Algorithm and Material Dispersion Implementation

Shawn W. Staker, Christopher L. Holloway, *Member, IEEE*, Alpesh U. Bhobe, and Melinda Piket-May, *Senior Member, IEEE*

***Abstract*—The alternating-direction implicit finite-difference time-domain (ADI-FDTD) technique is an unconditionally stable time-domain numerical scheme, allowing the Δt time step to be increased beyond the Courant–Friedrichs–Lewy limit. Execution time of a simulation is inversely proportional to Δt, and as such, increasing Δt results in a decrease of execution time. The ADI-FDTD technique greatly increases the utility of the FDTD technique for electromagnetic compatibility problems. Once the basics of the ADI-FDTD technique are presented and the differences of the relative accuracy of ADI-FDTD and standard FDTD are discussed, the problems that benefit greatly from ADI-FDTD are described. A discussion is given on the true time savings of applying the ADI-FDTD technique. The feasibility of using higher order spatial and temporal techniques with ADI-FDTD is presented. The incorporation of frequency dependent material properties (material dispersion) into ADI-FDTD is also presented. The material dispersion scheme is implemented into a one-dimensional and three-dimensional problem space. The scheme is shown to be both accurate and unconditionally stable.**

***Index Terms*—Alternating-direction implicit (ADI), ADI finite-difference time-domain (ADI-FDTD) method, FDTD, higher order schemes, material dispersion, unconditionally stable.**

I. Introduction

THE STANDARD finite-difference time-domain (FDTD) scheme is a well established technique for simulating electromagnetic (EM) systems. Two major limitations of FDTD are the simulation errors and execution time. The simulation errors are due to discretizing space and time, and are measured typically through the amount of numerical dispersion [1]. Long execution times result from the requirement of a time-domain signal to "ring out" or reach steady state.

The execution time of a FDTD simulation is inversely proportional to the size of the chosen time step. A major limitation of existing FDTD schemes is the conditionally stable nature of the technique. For stability of the FDTD scheme, one needs to ensure that

$$\Delta t < \frac{1}{v\sqrt{\frac{1}{\Delta x^2}+\frac{1}{\Delta y^2}+\frac{1}{\Delta z^2}}} \tag{1}$$

where v is the maximum speed of propagation in the computational volume, and Δx, Δy, and Δz are, respectively, the cell sizes in the x, y, and z directions. This criterion is referred to as the Courant or the Courant–Friedrichs–Lewy (CFL) stability condition [1], [2] and [3], and essentially states that the numerical speed of propagation must exceed the physical speed of propagation for numerical stability.

Obviously, to ensure a faster central processing unit (CPU) run time for the FDTD scheme, the time step Δt needs to be as large as the expression in (1) allows for numerical stability. From (1), it is seen that the maximum possible time step is based on the minimum required spatial cell size. The size of the spatial increment is governed by two requirements. First, the finite-difference grid should resolve the highest frequency of interest, which is accomplished usually by using at least 20 cells per wavelength at this frequency. Second, the cell's size should be small enough to ensure that all objects in the computational volume are spatially resolved by the cells. For low frequencies or small object dimensions, this second requirement is the most restrictive on Δh (where Δh represents any of the spatial cell sizes, i.e., Δx, Δy, or Δz) and can result in long computation times because of the CFL stability condition. Calculating scattering from an object with a thin material coating, lightning interaction with aircraft, modeling regions with noncubic cells with large aspect ratios (where Δt is governed by the smallest noncubic cell dimension), or propagation on transmission lines with conductors of small dimension are four examples where resolving the object (i.e., the thin material, the aircraft, source region modeling, or the conductors) gives a cell size much smaller than would be needed to resolve the frequency of interest. In these examples, the CFL bound on Δt leads to undesirable and often unrealistic execution times.

In order to solve these types of problems with time-domain difference techniques, a method for eliminating the CFL stability condition is desirable. The alternating-direction implicit (ADI) FDTD method, introduced by Namiki [4] and Zheng *et al.*[5], [6], is unconditionally stable. The ADI-FDTD scheme

Manuscript received July 15, 2002; revised January 3, 2003.

S. W. Staker is with the Department of Electromagnetics, Massachusetts Institute of Technology (MIT), Cambridge, MA 02139 USA.

C. L. Holloway is with the National Institute of Standards and Technology, RF Technology Division, U.S. Department of Commerce, Boulder Laboratories, Boulder, CO 80305 USA (email: holloway@boulder.nist.gov).

A. U. Bhobe and M. Piket-May are with Department of Electrical and Computer Engineering, University of Colorado, Boulder, CO 80302 USA.

Digital Object Identifier 10.1109/TEMC.2003.810815

allows Δt to be increased which can result in substantial reductions in the total execution time of numerical problems.

In this paper, various aspects of the ADI-FDTD scheme are discussed, including:

1) overview of the scheme;
2) defining the types of problem where ADI-FDTD is beneficial;
3) time savings of ADI-FDTD over FDTD;
4) higher order schemes;
5) introducing the implementation of frequency dependent materials (i.e., material dispersion).

The purpose here is to provide an understanding of where the ADI-FDTD scheme would be most beneficial in numerical EMC applications as well as presenting concepts which will expand the usefulness of the ADI-FDTD scheme in the EMC community.

II. Overview of the ADI-FDTD Scheme

The ADI technique is well reported in the study of parabolic equations [2]. The ADI technique takes its name from breaking up a single implicit time step into two half time steps. In the first half time step, an implicit evaluation is applied to one dimension and an explicit evaluation is applied to the other, assuming two dimensions in the problem statement. For the *second* half time step, the implicit and explicit evaluations are alternated, or switched, between the two dimensions. The dimensions to alternate between are typically spatial; however, temporal variables can also be used [7].

ADI as applied to the three-dimensional (3-D) FDTD technique was introduced by Zheng *et al.*[5], [6]. The ADI-FDTD method removes the CFL stability restraint, allowing any choice of Δt for a stable scheme. However, the accuracy is a function of Δt. Although any choice of Δt will be stable, the errors introduced may make some values unacceptable with respect to accuracy. It will be shown that the choice of Δt is determined by the required accuracy, and not by stability.

Any ADI scheme has the advantage of being unconditionally stable, and therefore implicit. ADI possess a significant advantage over other implicit schemes, i.e., the elimination of large matrix operations. The ADI-FDTD scheme forms tridiagonal, band-3 matrices, rather than the large nonbanded sparse matrices formed by other implicit schemes (which are computationally expensive to solve) [8]–[10]. Tridiagonal matrices have very simple and efficient solution techniques [2], [8]. ADI-FDTD requires less memory and possesses faster solution times than other implicit schemes, and retains the simplicity that is inherent in the traditional Yee FDTD technique [11].

The ADI-FDTD scheme requires splitting the full time step into two half time steps. Applying this procedure to Maxwell's equation results in a tridiagonal matrix for each of the E-field components. Once the E-field components are obtained, the H-field components are solved explicitly. The details for this type of formulation are found in [12]. The ADI-FDTD scheme as formulated in [5], [6], [12] has *second*-order accuracy in space and time, similar to the standard FDTD. The expression given in [12] assumes constant ε and μ. Slight variations are needed to include variable ε, and μ, and lossy material. A complete set of update equations for variable ε, and μ, and lossy material is found in [13].

Care must be taken in interpreting the field values at the half time steps. As explained in [8], the half time-step field values should not be treated as true field values. If one performs an accuracy analysis on the half time steps, one discovers that the half time-step quantities are only accurate to *first* order. It may be useful to reference the half time-step quantities as intermediate values, which must be re-combined with other quantities to be valid.

It is of interest to compare the accuracy of ADI-FDTD with that of the standard FDTD. ADI-FDTD uses central-difference formulas to evaluate both the time and space derivatives. These expressions are shown to be *second*-order accurate. However, since ADI-FDTD manipulates the temporal evaluations, the final accuracy, in time, may be an issue. To illustrate this, numerical dispersion for both FDTD and ADI-FDTD is investigated.

The amount of numerical dispersion in a scheme is directly correlated to the level of accuracy used in evaluating the derivatives. Thus a higher order central-difference formula would lead to lower dispersion error and more accurate results. A dispersion analysis can be viewed as a measure of the accuracy of all derivatives, time and space, taken together. A numerical dispersion analysis for the FDTD scheme is given in [1], and a dispersion analysis for the ADI-FDTD scheme in given in [14]. The results given in [14] for the ADI-FDTD dispersion analysis are for time steps (Δt) either greater or less than the CFL stability condition and does not give a direct comparison of ADI-FDTD and FDTD for a given Δt.

In order to obtain an assessment of the relative accuracy of the two different schemes, a dispersion analysis at the CFL limit is performed. Using the dispersion relations given in [1] and [14] a dispersion analysis for the two schemes was performed for a cubic cell (i.e., $\Delta h = \Delta x = \Delta y = \Delta z$) and for a temporal sampling set to the CFL stability constraint ($\Delta t = (\Delta h/v)\sqrt{3}$). In this analysis the spatial sampling as taken to be

$$\Delta h = \frac{\lambda_{\min}}{R}$$

where $\lambda_{\min}$ is the smallest possible wavelength of the source signal in the problem space. $R = 20$ is used here, and is the nominal spatial sampling used in most applications, because of the memory limitations in commonly used computers, and to create reasonable run times of simulations.

In this analysis, we find that FDTD has a maximum percentage error of 0.28%, while ADI-FDTD has a maximum percentage error of 0.69%. This illustrates that the ADI-FDTD scheme is less accurate than the FDTD scheme. However, both these errors are quite small, for most applications. The ADI-FDTD scheme as formulated in [5] and [6] is *second*-order accurate in space, and *second*-order accurate in time, similar to FDTD. However, a one-dimensional (1-D) analysis can show that the difference in the accuracy can be attributed to the fact that ADI-FDTD is not staggered in time, where FDTD is staggered in time [13].

We have shown that for the same spatial and temporal sampling, FDTD is more accurate, or the ADI-FDTD has a larger error term as compared to FDTD. The larger error term translates to more numerical dispersion for the same configuration. Following this, one would initially determine that a user must sacrifice accuracy for reduced run time. From an error perspective, it would appear that FDTD is a superior scheme compared to ADI-FDTD. For marginally resolved spatial problems, this is true. However there exists a class of problems for which ADI-FDTD gives a significant advantage over FDTD. For this class of the problem, ADI-FDTD greatly reduces the run times compared to FDTD. This class of problems is referred to as ADI-FDTD class problems.

III. Identification of ADI Class Problems

We begin the identification of this class of problems by setting a level of acceptable error. The obvious choice for this bound is the maximum percentage error of 0.28% resulting from FDTD when $R = 20$ and $\Delta t = \Delta t_{\mathrm{CFL}}$. If ADI-FDTD results in a shorter run time with an error less than or equal to 0.28%, ADI-FDTD will be considered to be a scheme superior to FDTD. The class of problems that fulfills this condition are systems that are over-resolved in space. This over-resolution in space can be a result of geometric features (as discussed in the introduction), lossy material, or other issues. Another class of problem that fulfills this condition is when noncubic cells with large aspect ratios are used (where Δt is governed by the smallest noncubic cell dimension). When the FDTD scheme is used on over-resolved problems (i.e., $R > 20$), the error is less than 0.28%. While the ADI-FDTD scheme has more error than the FDTD scheme, for over-resolved problems the error can be less than 0.28%. However, as Δt increases for over-resolved problems, the error also increases. A problem is identified as an ADI class problem if the application of ADI-FDTD results in decreased execution time (i.e., an increase in Δt) and the result also possesses an error level less than 0.28%.

In the analysis of identifying ADI class problems, we assume cubic cells ($\Delta h = \Delta x = \Delta y = \Delta z$) and define the spatial sampling as

$$\Delta h = \frac{\lambda_{\min}}{R} \tag{2}$$

where $\lambda_{\min}$ is the shortest wavelength in the problem space, and R is the spatial resolution in points per wavelength. Using the CFL condition given i.e., (1) and (2), the standard FDTD time step decreases as R increases by the following:

$$\Delta t_{\mathrm{CFL}} = \frac{\Delta h}{v\sqrt{3}} = \frac{\lambda_{\min}}{vR\sqrt{3}}. \tag{3}$$

For the purpose of introducing ADI class problems, consider a situation where a feature size forces a spatial resolution of $R = 200$. For this value of R and Δt, the numerical dispersion analysis gives an error greatly below the acceptable error level of 0.28%. The CFL bound forces an improvement in accuracy at the cost of longer execution time. If the improved accuracy is not required, which is usually the case, then the increase in execution time is prohibitive. ADI-FDTD has no CFL bound and as such Δt can be increased to a level that results in the acceptable error with a shorter execution time.

For problems that are over-resolved spatially, we are interested in determining how much larger the ADI-FDTD Δt can be increased over Δt_{CFL} while maintaining the same error of a standard FDTD scheme. To easily identify ADI class problems we need to derive a formula to estimate the amount of increase to Δt for a given R. This is accomplished by solving the numerical dispersion relation.

To find the amount by which Δt can be increased for a given R, we iteratively solve the numerical dispersion relation until we reach the value of Δt that gives the acceptable error. For cubic cells, we define the time step for ADI class problems that have the desired acceptable error as

$$\Delta t_{\mathrm{ADI}} = N\Delta t_{\mathrm{CFL}} = \frac{\Delta h}{v\sqrt{3}}\, N = \frac{\lambda_{\min}}{vR\sqrt{3}}\, N. \tag{4}$$

To estimate Δt_{ADI} we set the error to 0.28%, R to a given level, and solve for Δt. We repeat this process for a range of $R's$ and plot the trend in Fig. 1. From the curve in Fig. 1 we derive the relation

$$N \simeq \frac{R}{20}, \qquad \text{for } R \geq 100. \tag{5}$$

For example, let $R = 350$; from(4) and (5) we find a time step for ADI-FDTD that is 17.5 times greater than FDTD. Because ADI-FDTD is more computationally intensive compared to FDTD, increasing the time step by a factor of 17.5 does not reduce the execution time the same amount. The next section addresses this issue. Using (5) we can easily predict the amount of Δt increase while preserving the desired accuracy.

Combining (2), (4), and (5) into one equation yields

$$\Delta t_{\mathrm{ADI}} = \frac{\lambda_{\min}}{20v\sqrt{3}}. \tag{6}$$

From (6), we conclude that for ADI class problems the time step is independent of spatial sampling. The 20 in the denominator of (6) is the result of setting the acceptable error to 0.28% or $R = 20$ in FDTD. Setting the acceptable error level to FDTD with $R = 30$ yields $N \simeq R/30$ for (5). One could also interpret (6) as setting Δt_{ADI} equal to Δt_{CFL} with R at the resolution of acceptable error. In a recent paper [15], Zhao investigates the same issue of Δt requirements for a desired numerical dispersion accuracy. Zhoa takes a different approach and shows different types of results for time step versus accuracy for both uniform and nonuniform meshes. Zhoa does agree with our finding, in that the efficiency and accuracy of the ADI-FDTD scheme is significantly improved when the spatial sampling (R) is high.

This analysis in this section shows that the standard FDTD scheme time step is governed by the CFL, while the ADI-FDTD scheme is governed only by the accuracy one desires. Thus, the time saving can be tremendous, and the more over-resolved a problem is, the more the time is saved with the ADI-FDTD scheme. This feature of the ATD-FDTD scheme makes it well suited for a large set of EMC applications.

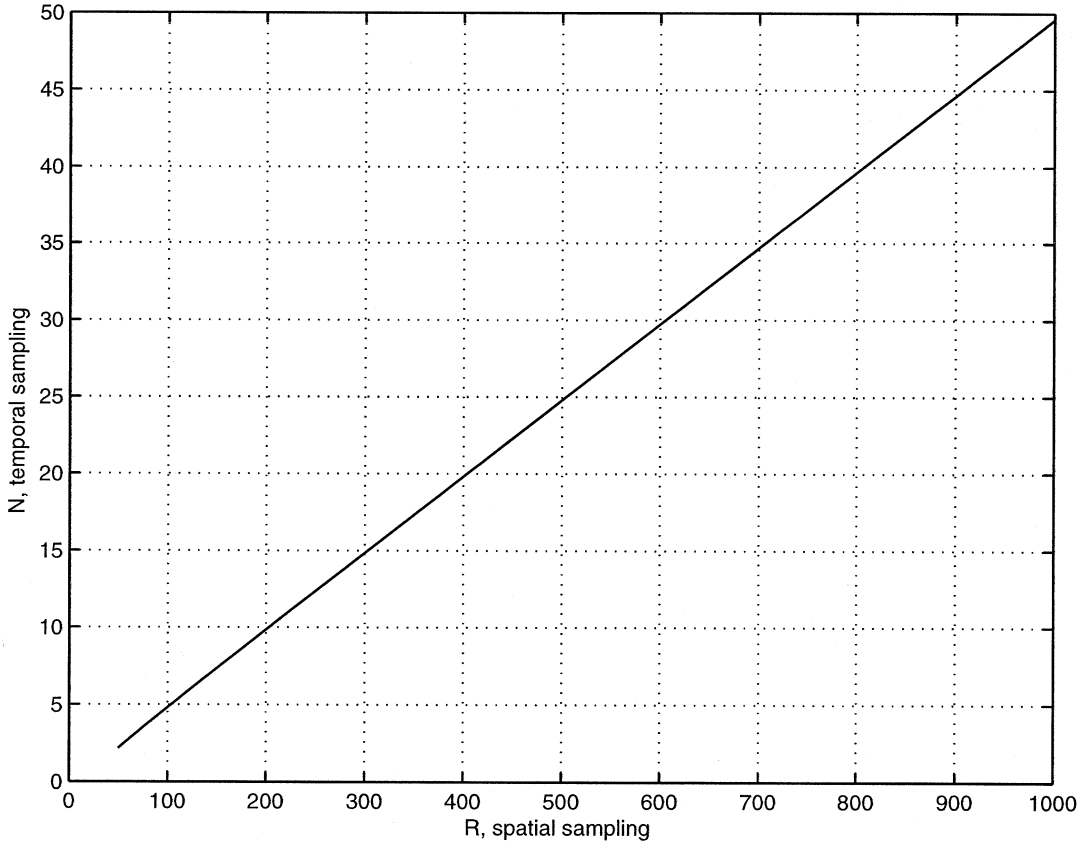

Fig. 1. Plot showing the bound on Δt as the spatial sampling is increased for the ADI-FDTD scheme.

IV. Estimating True Time Savings

Execution time is a function of the problem space being simulated, $\mathrm{Tot_{fp}}$, and the number of time steps, $n\max$

$$\text{execution time} = f_{\text{time}}\,(n\max,\ \mathrm{Tot_{fp}}) \tag{7}$$

where $\mathrm{Tot_{fp}}$ is the total number of field points in the problem space. Deriving a closed form expression for f_{time} is not feasible. f_{time} is highly dependent on the implementation style of the ADI-FDTD algorithm and on the machine used to execute the code. Because of this dependency, only an empirical form of f_{time} is presented.

ADI-FDTD splits each time step into two half time steps, resulting in more update equations per Δt. Also, the tridiagonal solver of ADI-FDTD is computationally more intensive than the explicit update of FDTD. To obtain an empirical expression for f_{time}, real FORTRAN code is timed out in operation. All computations in this section were performed on a SGI Octane, however it is noted that the following technique removes any dependency to a specific machine.

The execution time of a single Δt time step for an entire problem space is proportional to the total execution time and the number of unknowns in the problem space as

$$t_{\Delta t} \propto \frac{\text{total execution time}}{n\max}. \tag{8}$$

Equation (8) is essentially an average, where the accuracy increases with more time steps or $n\max$. Equation(8) was repeated with increasing $n\max$, until $t_{\Delta t}$ converged to a constant value. This process was repeated for increasing values of $\mathrm{Tot_{fp}}$, with the results summarized in Fig. 2. Fig. 2 reveals a linear relationship between $t_{\Delta t}$ and $\mathrm{Tot_{fp}}$ for large values of $\mathrm{Tot_{fp}}$.

The execution time can now be expressed as

$$\text{total execution time} = t_{\Delta t}(\mathrm{Tot_{fp}}) \cdot \mathrm{Tot_{fp}} \cdot n\max \tag{9}$$

where $t_{\Delta t}(\mathrm{Tot_{fp}})$ is an empirical function found from the curves in Fig. 2, and is linear for large values of $\mathrm{Tot_{fp}}$. Using (4), (5), and (9), we can calculate a time estimate for FDTD and ADI-FDTD. The difference between the two is an estimate of the true time savings for a problem, and is given as

$$\begin{aligned}\text{savings} = (t_{\text{sim}} v \mathrm{Tot_{fp}})[&t_{\Delta t\_\mathrm{FDTD}}(\mathrm{Tot_{fp}}) \\ &- 20 t_{\Delta t\_ADI}(\mathrm{Tot_{fp}})/R] \\ &\cdot \sqrt{(\Delta x)^{-2} + (\Delta y)^{-2} + (\Delta z)^{-2}}\end{aligned} \tag{10}$$

where t_{sim} is the required simulated time for the EM system, v is the maximum speed of propagation, and $t_{\Delta t\_\mathrm{FDTD}}$ and $t_{\Delta t\_\mathrm{ADI}}$ are empirical functions as given in Fig. 2.

An example will illustrate the simplicity and usefulness of (10). Given cubic cells, with $\Delta h = 1$ mm, $\lambda_{\min} = 0.5$ m, $t_{\text{sim}} = 9.6$ ns, and a $100 \times 100 \times 100$ problem space, (10) yields a savings of 20.32 h. Individual execution times are respectively 22.35 and 2.02 h for FDTD and ADI-FDTD. If the required simulation time is increased by a factor of 10, or $t_{\text{sim}} = 96$ ns, the resulting savings would be over 8 days.

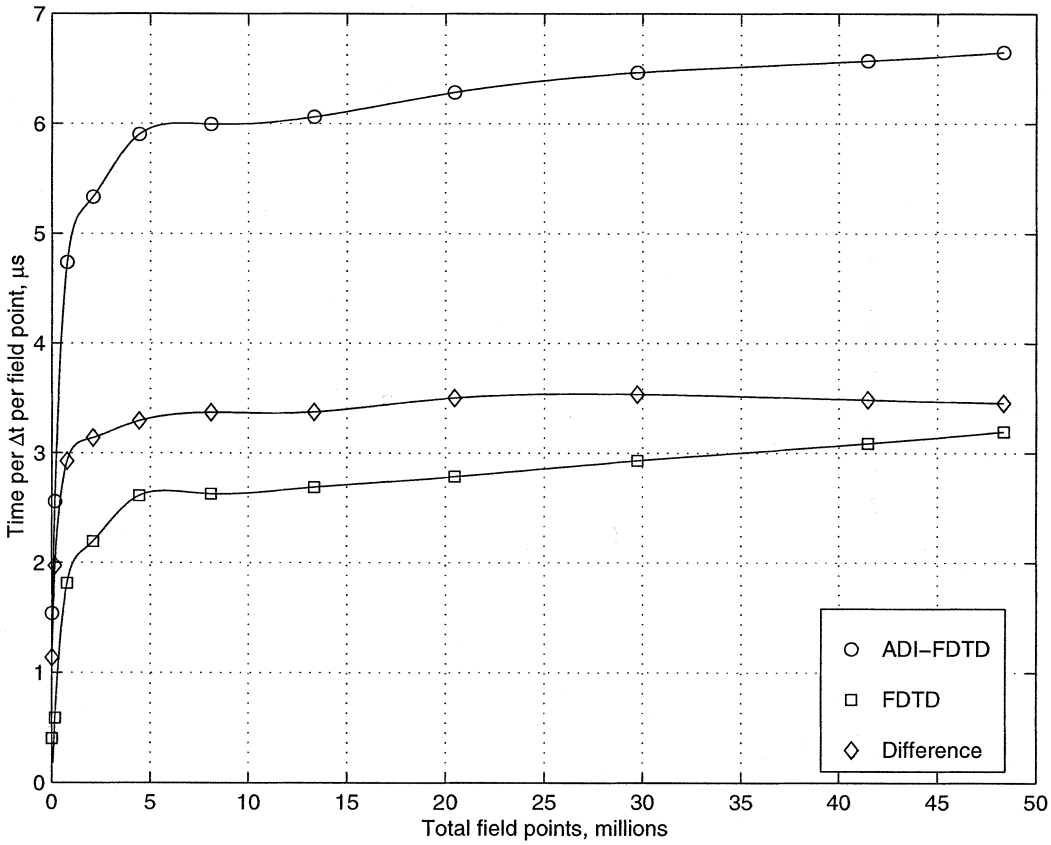

Fig. 2. Plot of the execution time for a single time step $t_{\Delta t}$ as a function of problem space $\mathrm{Tot}_{\mathrm{fp}}$.

From Section III we determined that a problem must be over resolved to take full advantage of the ADI-FDTD scheme. Equation (10) gives a measure of the advantage. It should be noted that (10) was developed for a vacuum problem space with perfect electric conductor (PEC) boundary conditions. To estimate the time savings for an ADI-FDTD code with other features one must calculate a new form for Δt_{ADI} and generate new curves in Fig. 2. It is also noted that though $t_{\Delta t\_\mathrm{FDTD}}$ and $t_{\Delta t\_\mathrm{ADI}}$ are machine dependent, the relative difference is not.

V. Higher Order ADI

A. Higher Order Spatial Schemes

Increasing spatial accuracy is a very direct way to improve the performance of a scheme. Expanding the spatial derivatives of ADI-FDTD in a *fourth*-order Taylor-series expansion results in a scheme accurate to *fourth* order in space, referred to as ADI-S24. A stability analysis, omitted here due to length restrictions, reveals ADI-S24 to be unconditionally stable (for detail see [13]). The expression for numerical dispersion provides a means to evaluate the scheme's performance relative to FDTD (the standard *second*-order space and time FDTD scheme) and ADI-S22 (formally referred to as ADI-FDTD). For coarse resolution, the dispersion error is dominated by Δt, which is unaffected by spatial accuracy. For over-resolved problem spaces we need to formulate a similar expression for N, as in (5). For ADI-S24 we find

$$N \simeq \frac{R}{20} + 0.1, \qquad \text{for } R \geq 100. \tag{11}$$

This is a very slight increase as compared to the N for ADI-S22. From (11), we can determine that higher order spatial ADI-FDTD schemes do slightly improve the associated dispersion error. However, this improvement comes with a cost of complexity and an increased time for a single Δt execution. The application of higher order spatial schemes to ADI class problems appears to provide no benefit to overall performance.

The lack of improvement from higher order spatial schemes to ADI-FDTD can be understood by returning to higher order FDTD schemes. To take advantage of the improved accuracy in the spatial domain, the temporal resolution must be increased [16]. Increasing temporal resolution is equivalent to decreasing the time step Δt. The power of ADI-FDTD lies in its ability to increase Δt, and thus reduce execution time. In every case where ADI-FDTD had superior performance as compared to FDTD, the Δt time step was increased. Because of this, higher order spatial schemes provide no benefit to ADI-FDTD for ADI class problems.

This conclusion is supported by (6). Equation (6) reveals ADI class problems to be independent of spatial sampling. To improve the accuracy of Δt_{ADI} one must increase accuracy in the temporal domain.

B. Higher Order Temporal Schemes

Higher order temporal derivatives may be used to improve the performance of ADI-FDTD. Candidates for higher temporal accuracy include direct expansion of ∂t, the "modified equation method" [17] [18], and multistep methods. Higher order Taylor expansions of ∂t for wave-type equations are inherently unstable [19]. The "modified equation method," and multistep methods are revealed to be inappropriate for ADI class problems.

The "modified equation method" transforms a higher order time derivative to a series of higher order mixed spatial derivatives. The numerical evaluation of a mixed derivative results in a stencil that spans more than one dimension. This characteristic will negate the use of the tridiagonal solver. The use of a tridiagonal solver allows the implicit formulation to be computational efficient. This is a subtle, but important point. The numerical derivatives of ADI-FDTD must be contained in one dimension. This fact also precludes the use of any modified higher order spatial schemes [13] and [16].

The combination of multistep methods with the method of lines, provides a convenient and powerful technique to evaluate higher order temporal derivatives. The goals in investigating higher order temporal schemes for ADI-FDTD applications can be grouped into two categories. First, we wish to increase the temporal accuracy in order to improve upon Δt_{ADI} in (6). This equation was developed by exploiting the unconditionally stable nature of ADI-FDTD. The parallel for multistep schemes is referred to as A-stable schemes. An A-stable multistep scheme would result in an unconditionally stable scheme for FDTD applications. The first Dahlquist stability barrier states that the highest order of accuracy for an A-stable multistep method is *second* order [19]. Essentially, it is theoretically impossible to improve on (6) using multistep methods.

The second objective of the temporal investigation is to find a more accurate scheme when the spatial sampling is moderately resolved, or non-ADI class problems. No multistep formulation was found which possess accuracy higher than *second* order with a stability domain beyond the CFL bound [13].

Higher order implicit Runge–Kutta (RK) methods have recently been applied to systems of equations, and result in an A-stable or unconditionally stable scheme. Implicit RK methods for systems of equations effectively require multiple time steps to be solved simultaneously, which may be computationally prohibitive. Research is presently being conducted on integrating implicit RK methods with ADI-FDTD.

VI. Material Dispersion Model

In many applications, electromagnetic fields encounter frequency-dependent materials (i.e., material dispersion). In order for the ADI-FDTD scheme to be useful for a general class of problems, it must be capable of handling material dispersion. A method for incorporating material dispersion into ADI-FDTD is presented in this section.

The method we have chosen to simulate the frequency dependence of the material is a *first*-order Debye model [20]. The following scheme is developed using the concept of magnetic polarizability with the Debye model. This approach can be generalized for electric losses as well [20].

The B field is given by

$$B = \mu H = \mu_o H + M \tag{12}$$

where $M = \mu_o H \chi_M$. M is referred to as the magnetization density and χ_M the magnetic susceptibility. The frequency dependence is given by a *first*-order Debye model as

$$\chi_M = \frac{\kappa_o}{1 + j\,\frac{\omega}{\omega_o}} \tag{13}$$

where κ_o and ω_o are constants representing the absorption peak and the relaxation frequency of the bulk material. This *first*-order Debye model is very accurate in modeling various materials, including ferrite tiles. By replacing the $j\omega$ with $\partial_t \equiv \partial/\partial t$, we obtain a time-domain operator relating the current time value of M to the previous time values of M and B. This process yields a partial differential equation (PDE) for M as

$$\partial_t M = \omega_o \kappa_o B - \omega_o \left(1 + \kappa_o\right) M. \tag{14}$$

It should be noted that loss mechanisms that behave differently than a simple first-order Debye model can be realized with a series of *first*-order Debye terms, see discussions in [20] and [21] for details.

A few comments are in order about the procedure used for incorporating the Debye model for frequency dependent materials. Since the B is given as a multiplication of μ and H in the frequency domain, it will result in a convolution in the time domain. Incorporating frequency dependence results in an evaluation of a convolution integral. The procedure presented here is an alternative to the conventional method for performing the convolution. This approach is essentially a differential form of the convolution which is equivalent to the integral form. However, this differential approach is easier to implement for certain materials [20]. There are other alternative methods for evaluating the convolution integral, for example the z-transform method [22], which like the differential approach, involves a manipulation of the convolution integral.

The challenge of developing an ADI-FDTD scheme with material dispersion involves formulating an update equation for M that is unconditionally stable. This is accomplished via a Crank–Nicolson approach. The Crank–Nicoloson technique is a well reported unconditionally stable numerical scheme [2]. Applying this scheme to the PDE in (14) yields a first subiteration update for M as

$$M_{i+1/2}^{n+1/2} = \left[\frac{\Delta t \omega_o \kappa_o}{4 + \Delta t \omega_o \left(1 + \kappa_o\right)}\right] \left(B_{i+1/2}^{n+1/2} + B_{i+1/2}^{n}\right) + \left[\frac{4 - \Delta t \omega_o \left(1 + \kappa_o\right)}{4 + \Delta t \omega_o \left(1 + \kappa_o\right)}\right] M_{i+1/2}^{n}. \tag{15}$$

For clarity, it is noted that M has three components to match the three components of B. The update equations for E and B are found following the same process as outlined in [13].

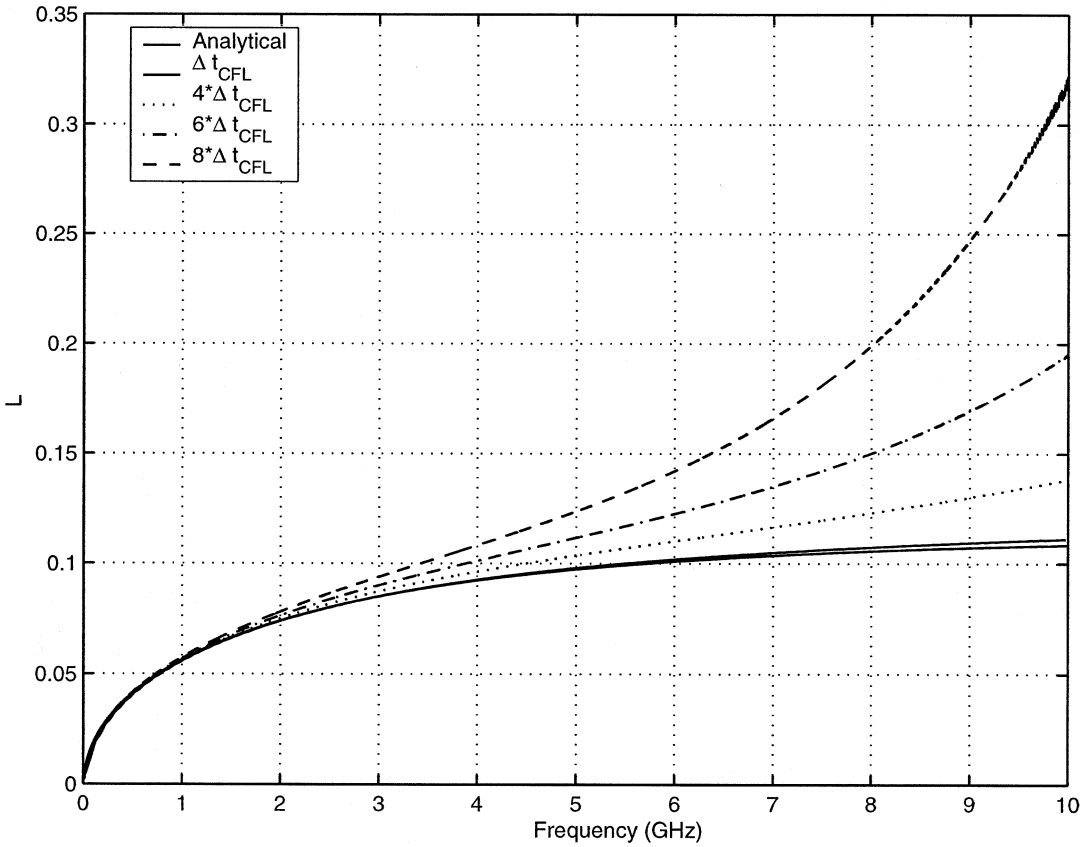

Fig. 3. Comparative error plots of ADI-FDTD with material dispersion, showing the resulting error as Δt increases.

A. 1-D Scheme

The PDE's that make up FDTD for the 1-D case are well known. When a *first*-order Debye model is included the resulting 1-D system is

$$\partial_t E = \frac{1}{\epsilon \mu_o}\, \partial_x (B - M) \tag{16}$$

$$\partial_t B = \partial_x E \tag{17}$$

$$\partial_t M = \omega_o \kappa_o B - \omega_o (1 + \kappa_o) M. \tag{18}$$

Applying the ADI technique yields two subiterations. For the 1-D case there are three equations per subiteration. We should note that in general, ϵ may be frequency dependent as well and a similar procedure can be followed to handle material dispersion in ϵ (see [20] and [21] for details). However, in order to simplify the discussion of the use of the Debye model in the ADI-FDTD scheme we concentrate only on frequency dependent μ. In addition, the examples shown here are for lossy ferrite materials, which are accurately represented by constant ϵ and frequency dependent μ [23].

To validate the 1-D scheme, we compare the analytical and numerical plane wave attenuation over a fixed distance as a function of frequency. Fig. 3 compares the analytical plane-wave loss [which we defined as $L = 1 - \exp(k_I d)$, where k_I in the imaginary part of the complex wave number in the medium and d is the distance the wave travels] with the loss obtained from the ADI-FDTD scheme for increasing values of Δt. The plane-wave loss is simply the difference in amplitude of the wave at a distance d from the incident amplitude (then normalized to the incident amplitude). The CFL stability constraint for a 1-D problem is $\Delta t_{\mathrm{CFL}} = \Delta x / v$, where v represents the maximum velocity in the medium [1]. All curves in Fig. 3 were calculated using $\kappa_o = 1101.7$ and $\omega_o = 2\pi 7.066 \cdot 10^6$, which is indicative of absorbing ferrite tile [20]. Fig. 3 validates the unconditionally stable performance of the ADI-FDTD scheme with material dispersion. As expected the accuracy decreases as the time step is increased and as frequency increases.

As discussed previously, ADI-FDTD is most beneficial when applied to over-resolved problem spaces, referred to as ADI class problems. By defining the spatial sampling by $\Delta x = \lambda_{\min}/R$ (where R is referred to as the spatial sampling), the CFL constraint is given by $\Delta t_{\mathrm{CFL}} = \lambda_{\min}/Rv$. Following similar arguments as above we find the time step for 1-D ADI class problems as

$$\Delta t_{\mathrm{ADI}} = \frac{\lambda_{\min}}{20v}. \tag{19}$$

From (19), we observe that for ADI class problems the time step is solely determined by temporal sampling.

Fig. 4 compares the analytical plane-wave loss [i.e., $L = 1 - \exp(k_I \Delta x)$] with the numerical loss obtained from ADI-FDTD for increasing values of R. From Fig. 4 we note that ADI-FDTD applied to over-resolved problems yields an increase in the time step while maintaining the acceptable level of accuracy. Fig. 4

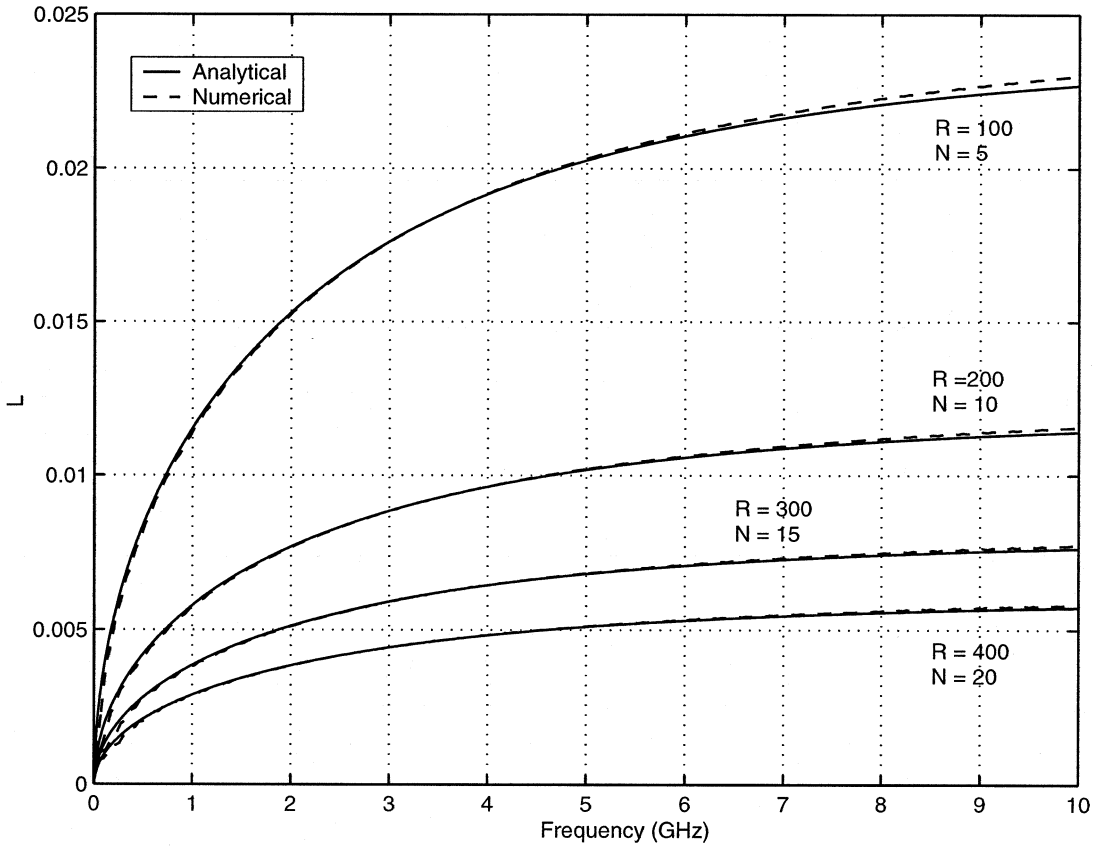

Fig. 4. Comparative error plots showing that ADI-FDTD with material dispersion retains the ability to accurately model ADI class problems.

validates ADI-FDTD with material dispersion as being applicable to ADI class problems. The purpose of the 1-D validation is to show the unconditionally stable performance of the technique, and to show the relative error performance that will follow in the 3-D case.

B. 3-D Scheme

The update for M is once again given in (15). Following the typical ADI-FDTD process the only field quantity solved implicitly are the E-field components [6]. With these new E-field values, the B and M quantities become explicit updates. Thus the only updates that need further explanation are the E-field ones.

The update equations may be obtained by substitutions or via a matrix approach. The matrix approach involves use of differential operators for each derivative. One then forms a matrix system for each subiteration. For example, the first subiteration would yield

$$[X]^{n+1/2} = [A][X]^n \tag{20}$$

where $[X]$ is a one-column vector containing E, B, and M at each Cartesian direction (the superscript on $[X]$ corresponds to the step index). $[A]$ is a square matrix of size [9 × 9]. From $[A]$, one may construct the continuous form of the E-field updates. To obtain the discrete updates, one evaluates the continuous derivatives with the correct numerical evaluation [13]. The complete tridiagonal update equation for the $E_x^{n+1/2}$ field is

$$\begin{aligned}
&-\left(C_a\frac{\Delta t^2}{4\mu\varepsilon\Delta y^2}\right)\cdot E_x|^{n+1/2}_{i+1/2,\,j+1,\,k} + \left(1+C_a\frac{\Delta t^2}{2\mu\varepsilon\Delta y^2}\right)\\
&\quad\cdot E_x|^{n+1/2}_{i+1/2,\,j,\,k} - \left(C_a\frac{\Delta t^2}{4\mu\varepsilon\Delta y^2}\right)\cdot E_x|^{n+1/2}_{i+1/2,\,j-1,\,k}\\
&= E_x|^{n}_{i+1/2,\,j,\,k} - \frac{\Delta t}{2\mu\varepsilon\Delta z}\cdot\Big(B_y|^{n}_{i+1/2,\,j,\,k+1/2}\\
&\quad - B_y|^{n}_{i+1/2,\,j,\,k-1/2} - M_y|^{n}_{i+1/2,\,j,\,k+1/2}\\
&\quad + M_y|^{n}_{i+1/2,\,j,\,k-1/2}\Big) + \left[\frac{4+\Delta t\omega_o\,(1-\kappa_o)}{4+\Delta t\omega_o\,(1+\kappa_o)}\right]\\
&\quad\cdot\left[\frac{\Delta t}{2\mu\varepsilon\Delta y}\right]\cdot\Big(B_z|^{n}_{i+1/2,\,j+1/2,\,k} - B_z|^{n}_{i+1/2,\,j-1/2,\,k}\Big)\\
&\quad - \left[\frac{4-\Delta t\omega_o\,(1+\kappa_o)}{4+\Delta t\omega_o\,(1+\kappa_o)}\right]\cdot\left[\frac{\Delta t}{2\mu\varepsilon\Delta y}\right]\\
&\quad\cdot\Big(M_z|^{n}_{i+1/2,\,j+1/2,\,k} - M_z|^{n}_{i+1/2,\,j-1/2,\,k}\Big) - C_a\\
&\quad\cdot\left[\frac{\Delta t^2}{4\mu\varepsilon\Delta y\Delta x}\right]\cdot\begin{pmatrix} E_y|^{n}_{i+1,\,j+1/2,\,k} - E_y|^{n}_{i,\,j+1/2,\,k}\\ -E_y|^{n}_{i+1,\,j-1/2,\,k} + E_y|^{n}_{i,\,j-1/2,\,k}\end{pmatrix}
\end{aligned} \tag{21}$$

where

$$C_a = \frac{4+\Delta t\omega_o}{4+\Delta t\omega_o(1+\kappa_o)}. \tag{22}$$

TABLE I
RESULTS VALIDATING THE UNCONDITIONAL NATURE OF THE PROPOSED 3-D ADI-FDTD MATERIAL DISPERSION SCHEME

FDTD	ADI-FDTD			
Δt_{CFL}	Δt_{CFL}	$4\Delta t_{CFL}$	$6\Delta t_{CFL}$	$8\Delta t_{CFL}$
Result (MHz)	Result (MHz)	Result (MHz)	Result (MHz)	Result (MHz)
14.5	14.48	14.26	13.59	11.32

If κ_o is equal to zero, the medium is frequency independent and (21) reduces to the standard ADI-FDTD update equation.

We employed the cavity-resonance problem as described in [6] as a validation model. We set $\Delta x = \Delta y = \Delta z = 0.1$ m, and used a problem space of $10 \times 20 \times 15$ cells. For ease we completely filled the metallic cavity with a dielectric of $\epsilon_r = 64$. For a nondispersive cavity, the CFL time step was found to be 1.54 ns. The fundamental resonant frequency was found analytically to be 15.6 MHz.

The first validation is to set $\kappa_o = 0$, which effectively gives a nondispersive material. Using the CFL time step. we found a numerical resonance at 15.6 MHz. Increasing the κ_o by a small amount introduced a proportionally small amount of dispersive loss. Setting $\kappa_o = 0.1$ and $\omega_o = 2\pi 7.066 \cdot 10^6$ yielded a numerical resonance at 15.47 MHz. This is in close agreement with the analytical estimate of 15.48 MHz. The analytical estimate was obtained by inserting the complex form of μ_r into the analytical expression of a homogeneous filled metallic cavity, and taking the real part. This estimate begins to deviate from the true resonance as the dispersive losses increase.

The 3-D case was also validated by comparing results of the material-dispersion model implemented into the standard FDTD scheme. The *first*-order Debye model was implemented into a standard FDTD scheme as reported in [20]. For the results in Table I, we set $\kappa_o = 1$, $\omega_o = 2\pi 7.066 \cdot 10^6$, and $\epsilon_r = 64$. As before the cells are cubic with 0.1 m dimension. The CFL for this problem space was found to be $\Delta t_{\mathrm{CFL}} = 1.83$ ns. From Table I we conclude that 3-D ADI-FDTD with material dispersion is unconditionally stable. The problem for Table I is not an ADI class problem and as such we expect the decrease in accuracy as Δt increases.

In the next example, we investigate a inhomogeneous filled cavity with dimensions of $60 \times 60 \times 40$ mm. Half the cavity was filled with a lossy material with $\kappa_o = 1101.4$, $\omega_o = 2\pi 3.55 \cdot 10^6$, and $\epsilon_r = 1$ and the other half is filled with a lossless material with $\mu_r = 1$ and $\epsilon_r = 1$. The resonance frequency for the cavity was determined with a standard FDTD code to be 3.22 GHz; with a ADI-FDTD code, the resonance frequency was determined be 3.22, 3.23, 3.25, and 3.28 GHz for $\Delta t_{\mathrm{ADI}} = \Delta t_{\mathrm{CFL}}$, $\Delta t_{\mathrm{ADI}} = 2\Delta t_{\mathrm{CFL}}$, $\Delta t_{\mathrm{ADI}} = 4\Delta t_{\mathrm{CFL}}$, and $\Delta t_{\mathrm{ADI}} = 6\Delta t_{\mathrm{CFL}}$, respectively. These results illustrate that the ADI-FDTD can accurately handle discontinuity of lossy materials (i.e., inhomogeneous media). The next example also illustrates this point for thin lossy materials.

For a final example, the time-domain and frequency-domain results of the E field inside a metal cavity with a layer of magnetic material 5 mm thick on the walls was investigated. For the magnetic material we used $\kappa_o = 550.7$ and $\omega_o = 2\pi 7.066 \cdot 10^6$. In this example, we will illustrate that even when the problem space in not over-resolved, ADI-FDTD will give results that are not only comparable to the FDTD results but are also stable for $\Delta t > \Delta t_{\mathrm{CFL}}$. Fig. 5 shows the time-domain waveform of the E field for a differential Gaussian pulse source placed in the center of the cavity. This figure compares the results of the FDTD scheme to the results of the ADI-FDTD scheme for $\Delta t = 4\Delta t_{\mathrm{CFL}}$ and $\Delta t = 6\Delta t_{\mathrm{CFL}}$. Since the metal cavity is lined with the lossy thin layer of magnetic material, the amplitude of the E field damps down fairly quickly. Notice that the amplitude of the waveform obtained from ADI-FDTD starts to differ from the FDTD results for $\Delta t > \Delta t_{\mathrm{CFL}}$; however, the ADI-FDTD are stable for $\Delta t > \Delta t_{\mathrm{CFL}}$. Fig. 6 shows the magnitude of the frequency-domain E field. This figure also compares

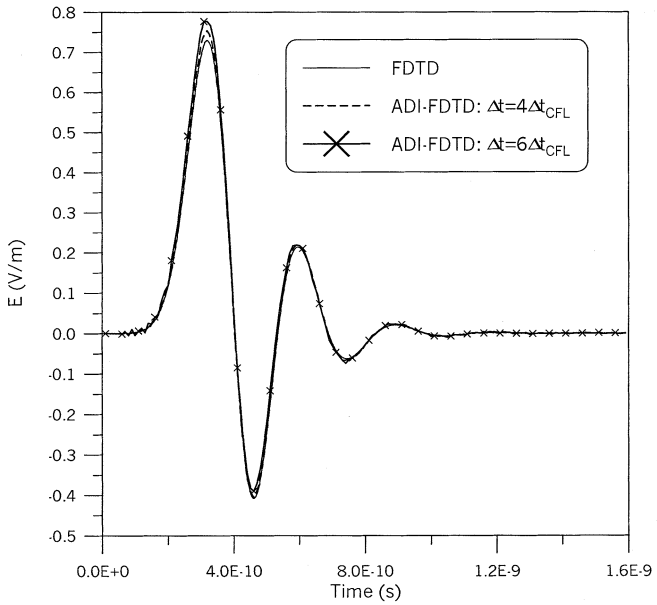

Fig. 5. Comparison of the time-domain E-field waveform in a lossy cavity obtained from FDTD and ADI-FDTD.

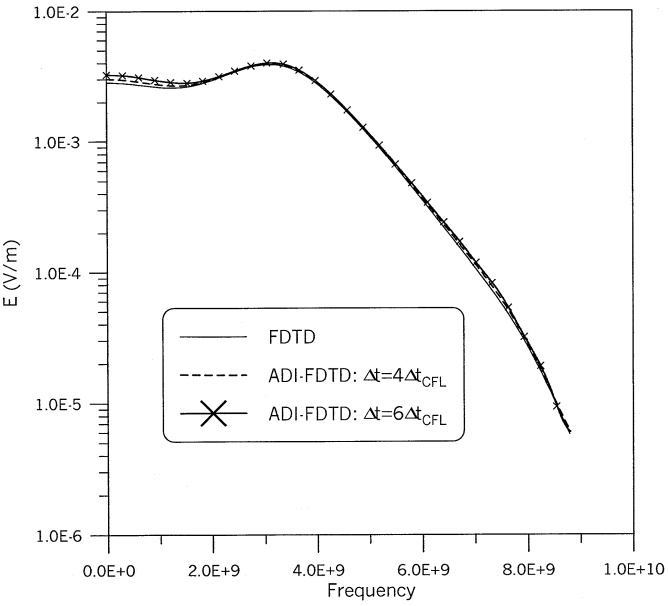

Fig. 6. Comparison of the E field as a function of frequency in a lossy cavity obtained from FDTD and ADI-FDTD.

the results of the FDTD scheme to the results of the ADI-FDTD scheme for $\Delta t = 4\Delta t_{\rm CFL}$ and $\Delta t = 6\Delta t_{\rm CFL}$.

In all these examples presented here, we have shown that the ADI-FDTD scheme can substantially reduce the run-time, while maintaining the desired accuracy level.

VII. Discussions and Conclusions

ADI-FDTD has been reported as a means to increase Δt at the cost of accuracy [6]. In this paper, ADI-FDTD has been revealed as a means to decrease a simulation's execution time while fully preserving accuracy. Problems that benefit the most from ADI-FDTD where identified and referred to as ADI class programs. These types of problems include problems that are over-resolved in space and problems where noncubic cells with large aspect ratios are used. An empirical formula was presented that gives a bound on Δt for ADI class problems. The accuracy of ADI class problems was shown to be independent of spatial sampling. Higher order spatial ADI-FDTD schemes were shown to provide no benefit to ADI class problems. However, higher order temporal variants have the potential to improve performance for ADI-FDTD. An implicit RK technique is presently being investigated as a candidate for a higher order temporal ADI-FDTD scheme.

The ability to incorporate material dispersion into ADI-FDTD was presented in this paper. A *first*-order Debye model was used to represent the frequency dependent material properties. The scheme was implemented into a 1-D and 3-D problem space. The scheme is shown to be both accurate and unconditionally stable. Higher order Debye and Lorentz models of material dispersion are presently being investigated.

ADI class problems result in a reduced run-time, while maintaining the desired accuracy level. There are various ADI class problems that exist in the EMC community, making the ADI-FDTD scheme a numerical technique that will be valuable for years to come.

Acknowledgment

The authors wish to thank P. McKenna, Institute for Telecommunication Sciences, U.S. Dept. of Commerce, for applying the standard FDTD result for the lossy cavity; and T. A. Driscoll for useful discussions.

References

[1] A. Taflove, *Computational Electrodynamics*. Norwood, MA: Artech House, 1995.

[2] G. D. Smith, *Numerical Solution of Partial Differential Equations*. Oxford, U.K.: Oxford Univ. Press, 1978.

[3] A. Taflove and M. E. Brodwin, "Numerical solution of steady-state electromagnetic scattering problems using the time-dependent Maxwell's equation," *IEEE Trans. Microwave Theory Tech.*, vol. MTT-23, pp. 623–630, Aug. 1975.

[4] T. Namiki, "A new FDTD algorithm based on alternating-direction implicit method," *IEEE Trans. Microwave Theory Tech.*, vol. 47, pp. 2003–2007, Oct. 1999.

[5] F. Zheng, Z. Chen, and J. Zhang, "A finite-difference time-domain method without the Courant stability conditions," *IEEE Microwave Guided Wave Lett.*, vol. 9, pp. 441–443, Nov. 1999.

[6] ——, "Toward the development of a three-dimensional unconditionally stable finite-difference time-domain method," *IEEE Trans. Microwave Theory Tech.*, vol. 48, pp. 1550–1558, Sept. 2000.

[7] T. Namiki and K. Ito, "A new FDTD algorithm free from the CFL condition restraint for a 2D-TE wave," in *Dig. 1999 IEEE Antennas and Propagation Symp.*, vol. 1, Orlando, FL, July 1999, pp. 192–195.

[8] J. C. Strikwerda, *Finite Difference Schemes and Partial Differential Equations*. Pacific Grove, CA: Brooks/Cole , 1989.

[9] R. L. Burden and J. D. Faires, *Numerical Analysis*. Pacific Grove, CA: Brooks/Cole, 1997.

[10] A. Iserles, *A First Course in the Numerical Analysis of Differential Equations*. New York: Cambridge Univ. Press, 1996.

[11] K. S. Yee, "Numerical solution of initial boundary value problems involving Maxwell's equations in isotropic media," *IEEE Trans. Antennas Propagat.*, vol. AP-14, pp. 302–307, May 1966.

[12] A. Taflove and S. C. Hagness, *Computational Electrodynamics*, 2nd ed. Norwood, MA: Artech House, 2000, pp. 160–172.

[13] S. Staker, "An algorithm study of the alternating direction implicit (ADI) technique applied to finite difference time domain (FDTD) schemes for electromagnetic applications," Master's thesis, Dep. Elect. Eng., University of Colorado, Boulder, CO, 2000.

[14] F. Zheng and Z. Chen, "Numerical dispersion analysis of the unconditionally stable 3-d ADI-FDTD method," *IEEE Trans. Microwave Theory Tech.*, vol. 49, pp. 1006–1009, May 2001.

[15] A. Zhao, "The influence of the time step on the numerical dispersion error of an unconditionally stable 3-d ADI-FDTD method: A simple and unified approach to determine the maximum allowable time step required by a desired numerical dispersion accuracy," *Microwave Opt. Technol. Lett.*, vol. 35, no. 1, pp. 60–65, 2002.

[16] M. F. Hadi, "A modified FDTD (2, 4) scheme for modeling electrically large structures with high phase accuracy," Ph.D. dissertation, Dep. Elect. Eng., University of Colorado at Boulder, Boulder, CO, 1992.

[17] G. Cohen and P. Joly, "Fourth order schemes for the heterogeneous acoustics equation," *Comp. Methods App. Mech. Eng.*, vol. 80, pp. 397–407, 1990.

[18] ——, "Construction analysis of fourth-order finite difference schemes for the acoustics wave equation in nonhomogeneous media," *SIAM J. Numer. Anal.*, vol. 33, no. 4, pp. 1266–1302, 1996.

[19] B. Fornberg, *A Practical Guide to Pseudospectral Methods*. New York: Cambridge Univ. Press, 1998.

[20] C. L. Holloway, P. McKenna, R. Dalke, R. Perala, and C. Devor, "Time-domain modeling, characterization and measurements of anechoic and semi-anechoic electromagnetic test chambers," *IEEE Trans. Electromagn. Compat.*, vol. 44, pp. 102–118, Feb. 2002.

[21] A. Scarlatti and C. L. Holloway, "An equivalent transmission line model for high speed digital transmission lines," *IEEE Trans. Electromagn. Compat.*, vol. 43, pp. 504–514, Nov. 2001.

[22] D. M. Sullivan, "Z-transform theory and the FDTD method," *IEEE Trans. Antennas Propagat.*, vol. 44, pp. 28–34, Jan. 1996.

[23] C. L. Holloway, R. R. DeLyser, R. F. German, P. McKenna, and M. Kanda, "Comparison of electromagnetic absorbers used in anechoic and semi-anechoic chambers for emissions and immunity testing of digital devices," *IEEE Trans. Electromagn. Compat.*, vol. 39, pp. 33–47, Feb. 1997.

Shawn W. Staker received the M.S. degree in electrical engineering from the University of Colorado, Boulder, in 2000. He is currently working toward the Ph.D. degree in computational electromagnetics at Massachusetts Institute of Technology (MIT), Cambridge.

He has worked in the Systems and Analysis division of MIT's Lincoln Laboratory.

Christopher L. Holloway (S'86–M'92) was born in Chattanooga, TN, on March 26, 1962. He received the B.S. degree from the University of Tennessee, Chattanooga, in 1986, and the M.S. and Ph.D. degrees from the University of Colorado, Boulder, in 1988 and 1992, respectively, both in electrical engineering.

During 1992, he was a Research Scientist with Electra Magnetic Applications, Inc., Lakewood, CO. His responsibilities included theoretical analysis and finite-difference time-domain modeling of various electromagnetic problems. From the fall of 1992 to 1994, he was with the National Center for Atmospheric Research (NCAR), Boulder, CO. While at NCAR, his duties included wave propagation modeling, signal processing studies, and radar systems design. From 1994 to 2000, he was with the Institute for Telecommunication Sciences (ITS), U.S. Department of Commerce, Boulder, CO, where he was involved in wave propagation studies. Since 2000, he has been with the National Institute of Standards and Technology (NIST), Boulder, CO, where he works on electromagnetic theory. He is also on the Graduate Faculty at the University of Colorado, Boulder. His research interests include electromagnetic field theory, wave propagation, guided wave structures, remote sensing, numerical methods, and EMC/EMI issues.

He is a member of Commission A of the International Union of Radio Science and an Associate Editor for the IEEE TRANSACTIONS ON ELECTROMAGNETIC COMPATIBILITY. Dr. Holloway was awarded the 1999 Department of Commerce Silver Medal for his work in electromagnetic theory and the 1998 Department of Commerce Bronze Medal for his work on printed circuit boards. He is the chairman for the Technical Committee on Computational Electromagnetics (TC-9) of the IEEE Electromagnetic Compatibility Society.

Alpesh U. Bhobe was born in Mumbai, India. He received the B.E. degree in electronics and telecommunications from the University of Bombay, Mumbai, India, in 1996, and the M.S. degree in electrical engineering from the University of Colorado, Boulder in 1999, where he is currently working toward the Ph.D. degree in electrical engineering.

Since August 1997, he has been working as a Research Assistant at the University of Colorado. His research interests include antenna designs, theoretical analysis, and finite-difference time-domain modeling of various electromagnetic problems.

Melinda Piket-May (S'89–M'92–SM'99) received the B.S.E.E. from the University of Illinois at Urbana-Champaign in 1988, and the M.S.E.E. and Ph.D. degrees in electrical engineering from Northwestern University, Evanston, IL, in 1990 and 1993, respectively.

Her work experience includes internships at Northwestern Memorial Hospital, Evanston, IL, Fermi National Accelerator Laboratory, Batavia, IL, Naval Research Laboratory, Monterey, CA, and Cray Research, Minneapolis, MN, as well as developing a number of educational programs. She joined the Electical and Computer Engineering Department at the University of Colorado, Boulder in 1993, where she is currently an Associate Professor of Electrical and Computer Engineering and serves as the Associate Vice-Chancellor of Research. She has an active research program in computational electromagnetics. Her research is industrial based with applications in biomedical engineering, assistive technology, high-speed analog and digital design, signal integrity, EMC/EMI, solar cell design, and wireless communication. She is also very active in engineering education. Her focus is on moving toward an interactive environment where the student is in charge of the learning. She works on undergraduate engineering design issues and incorporating research into the classroom in an interactive and meaningful way.

Prof. Piket-May served on the Administrative Committee of the IEEE Antennas and Propagation Society (APS) (1998–2001), as an Associate Editor of IEEE TRANSACTIONS ON ANTENNAS AND PROPAGATION (1998–2002), and is currently a member of the IEEE Education Society Administrative Council (2001–2003) and an Associate Editor for IEEE AWPL. She received the 1996 URSI Young Scientist Award and was named a Sloan New Faculty Fellow in 1997. She was awarded a National Science Foundation CAREER Award in 1997, the 1999 ASEE Helen Plant Award, and the 2000 University of Colorado College of Engineering Peebles Teaching Award. In 2001–2002, she has been named a Pew Fellow as a part of the Carnegie Foundation Academy for Teaching and Learning (CASTLE). In 2001–2002, she was selected to be an Emerging Leaders Fellow for the University of Colorado and in 2002, was chosen as the first NSF CU-LEAP Fellow. She will be General Chair of the Frontiers in Engineering Education conference in November 2003.